NASA CASE NO. LAR 14779-1

PRINT FIG. 2

NOTICE

The invention disclosed in this document resulted from research in aeronautical and space activities performed under programs of the National Aeronautics and Space Administration. The invention is owned by NASA and is, therefore, available for licensing in accordance with the NASA Patent Licensing Regulation (14 Code of Federal Regulations 1245.2).

To encourage commercial utilization of NASA-owned inventions, it is NASA policy to grant licenses to commercial concerns. Although NASA encourages nonexclusive licensing to promote competition and achieve the widest possible utilization, NASA will provide the necessary incentive to the licensee to achieve early practical application of the invention. Address inquiries and all applications for license for this invention to **NASA Patent Counsel, Langley Research Center, Code 143, Hampton, Virginia 23665-5225.**

Serial No.: 07/885,714
05-14-92

LaRC

(NASA-Case-LAR-14779-1) MULTIRESPONSE IMAGER AND IMAGING PROCESS FOR IMPROVED RESOLUTION Patent Application (NASA) 16 p

N92-29951

Unclas
G3/74 0111105

NASA Case No. LAR 14779-1

AWARDS ABSTRACT

MULTIRESPONSE IMAGER AND IMAGING PROCESS FOR IMPROVED RESOLUTION

Image systems including television cameras, charge coupled device imagers, forward locking infrared sensors, and infrared detectors produce a video image that has a resolution limited by the sampling interval, i.e., the space between photodetectors, of the imager. Attempts to produce images of objects requiring a resolution greater than this sampling interval result in poor visual quality, aliasing, blurring, colored noise and ringing. Multiple representations to overcome this resolution limitation are often precluded since often only a single incident is available.

The implementation of this invention consists of two elements, the image-gathering device and an image-restoration filter algorithm. The image-gathering device is implemented with an optical aperture control that allows one to change the spatial-frequency response of the image-gathering device for each one of the A successive image acquisitions, and the image-restoration algorithm unscrambles the aliased and blurred signal components in the presence of photosensor noise to produce an image with an increased resolution. The upper limit of the increase in resolution is $1/\sqrt{A}$ times the sampling interval of the image-gathering device. The image-gathering device and the target should be stationary with respect to each other during the image-gathering process.

Novel aspects of the invention include assigning successive image acquisitons, unique spatial-frequency responses and then employing an image-restoration algorithm to unscramble the image based on these unique responses.

Inventors: Carl E. Fales, Fredrich O. Huck
Address: 18 S. Madison Lane, Newport News, VA 23606; 83 Linda Drive, Newport News, VA 23602
SS: [redacted]; SS: [redacted]
Employer: NASA LaRC
Initial Evaluator: Harry F. Benz

Serial No.: 07/885,714
Filed: May 14, 1992

07/585,714
05/14/92

MULTIRESPONSE IMAGE GATHERING AND PROCESSING FOR IMPROVED RESOLUTION

Origin of the Invention

The invention described herein was made by employees of the United States Government and may be manufactured and used by or for the Government for governmental purposes without the payment of any royalties thereon or therefor.

Background of the Invention

1. Technical Field

The present invention relates generally to image gathering and restoration. Multiresponse image gathering and digital restoration are combined for improved resolution.

2. Discussion of the Related Art

Image systems including television cameras, charge coupled device imagers, forward looking infrared sensors, and infrared detectors produce a video image that has a resolution limited to the sampling interval (space between photodetectors) of the imager. Hitherto, it has never been possible to produce images of the random objects commonly encountered in nature with a resolution that is finer than the sampling interval or, stated differently, with a spatial frequency that is higher than the sampling passband, or Nyquist frequency, of the imager.

The performance of conventional imaging is, in general, critically constrained by its sampling passband, spatial-frequency response, and sensitivity. These constraints limit the resolution of the restored images to the sampling interval, and further degrade their visual quality by blurring, aliasing artifacts, colored noise, and ringing. In some applications, e.g., planetary exploration, military reconnaissance or medical diagnosis, image gathering may be limited to a single costly event. Accordingly, the image gathering constraints need to be rigorously

accounted for without undue regard given to the complexity of processing required to do so.

Objects of the Invention

It is accordingly an object of the present invention to improve the spatial resolution of digitally restored images that can be attained by image gathering and digital restoration. The improvement is attained by unscrambling, within the presence of photosensor noise, the within sampling-passband and aliased signal components of several images, each acquired with a different spatial-frequency response.

Summary of the Invention

In this invention, the resolution is improved to be finer than the sampling interval of the imager or, stated differently, the spatial frequency is improved to be higher than the sampling passband of the imager. The imaging process consists of two steps. The first step consists of acquiring $\mathcal{A}$ images with the image-gathering device. Each one of the $\mathcal{A}$ images is obtained with a different spatial-frequency response relative to the sampling passband. Two conditions must be fulfilled during this step. One condition is that the image-gathering device and the target are stationary with respect to each other during the image-gathering process. The other condition is that the $\mathcal{A}$ different spatial-frequency responses extend beyond the sampling passband. It is a natural consequence of this image-gathering process that sufficiently sampled, i.e., within sampling-passband, signal components and insufficiently sampled, i.e., aliased, signal components are weighted differently and predictably.

The second step is to unscramble the within sampling-passband and aliased signal components and to restore these components as an image. The unscrambling and restoration is done in a single process. The Wiener-matrix filter (described below) restores an image with a restoration that is finer than the sampling interval by a factor of up to $1/\sqrt{\mathcal{A}}$ or, stated differently, it restores an image with a spatial

frequency that is higher than the sampling passband by a factor of up to $\sqrt{\mathcal{A}}$. The Wiener-matrix filter accounts for the aliasing, blurring and noise of the image-gathering process to restore an image with the minimum possible mean square error between the restored image and the actual target.

Brief Description of the Drawings

FIG. 1(a) is a representation of a two-dimensional narrow passband Wiener spectrum;

FIG. 1(b) is a representation of a two-dimensional, circularly symmetric and monotonically decreasing Wiener spectrum;

FIG. 2 is a schematic representation of the multi-response imaging process according to the present invention;

FIG. 3 is a representation of a multiresponse undersampled signal spectrum;

FIGS. 4(a), 4(b) and 4(c) graph typical spatial frequency response relative to the sampling passband when $\mathcal{A} = 1$, 4, and 9, respectively;

FIGS. 5(a), 5(b) and 5(c) graph typical through put responses relative to the sampling passband when $\mathcal{A} = 1$, 4, and 9, respectively, with an SNR = 256;

FIG. 6(a) is a random polygon target with a mean spatial detail of $\mu = 0.75$;

FIGS. 6(b), 6(c) and 6(d) are images of the target of FIG. 6(a) for $\mathcal{A} = 1$, 4, and 9 with SNR = 256;

FIG. 7(a) is a resolution wedge target; and

FIGS. 7(b), 7(c), and 7(d) are images of the target of FIG. 7(a) for $\mathcal{A} = 1$, 4, and 9 with SNR = 256.

Detailed Description of the Invention

FIG. 1(a) and (b) illustrate two examples of undersampling. Here (X, Y) are the rectangular lattice spacings, and (υ, ω) are spatial frequencies. The sampling passband is the dashed rectangular region bounded by the Nyquist frequencies, i.e., $|\upsilon| \leq 1/2X, |\omega| \leq 1/2Y$. The solid oval boundary describes the extent of the signal Wiener spectrum, and the dashed region represents the portion of

this spectrum that has been aliased into the passband. Consider first the narrow bandpassed spectrum shown in FIG. 1(a). There the aliased portion intuitively represents useful information: for, by a priori knowledge suggesting careful imaging and linear filtering, this part of the signal can be placed back to its original position and added to the portion within the passband to recapture the original signal, to the extent that the additive noise allows. This process places both the within-passband and the aliased regions of the signal on equal footing as useful information. Formulations that treat the aliased signal as noise would not capture the essence of this Wiener spectrum. Consider next the circularly symmetric and monotonically decreasing Wiener spectrum shown in FIG. 1(b). There the overlapping portions of the within-passband and aliased signals interfere with each other. If the within-passband and aliased signals cannot be unscrambled, then the aliased portion intuitively represents additive noise, i.e., information that is not only lost forever but also contaminates the within-passband signal, consistent with formulations that treat the aliased signal as noise.

However, this invention presents a method for unscrambling the within-passband and aliased signal components and restoring an image with a resolution that is finer than the sampling interval of the imager or, stated differently, with a spatial frequency that is higher than the sampling passband of the imager. The imaging process consists of two steps. The first step consists of acquiring $\mathcal{A}$ images with the image-gathering device. Each one of the $\mathcal{A}$ images is obtained with a different spatial-frequency response, or modulation transfer function, relative to the sampling passband. Two conditions must be fulfilled during this step. One condition is that the image-gathering device and the target are stationary with respect to each other during the image-gathering process. The other condition is that the $\mathcal{A}$ different spatial-frequency responses extend beyond the sampling passband. It is a natural consequence of this image-gathering process that sufficiently sampled, i.e., within sampling-passband, signal components and insufficiently sampled, i.e., aliased, signal components are weighted differently and predictably.

The second step is to unscramble the within sampling-passband and aliased signal components and to restore these components as an image. The unscrambling and restoration is done in single process. The Wiener-matrix filter (described

below) restores an image with a restoration that is finer than the sampling interval by a factor of up to $1/\sqrt{\mathcal{A}}$ or, stated differently, it restores an image with a spatial frequency that is higher than the sampling passband by a factor of up to $\sqrt{\mathcal{A}}$. The Wiener-matrix filter accounts for the aliasing, blurring and noise of the image-gathering process to restore an image with the minimum possible mean square error between the restored image and the actual target.

FIG. 2 is a simplified schematic diagram of the multiresponse image-gathering and Wiener-matrix restoration process. Thus, as illustrated in FIG. 3, each signal $s_\alpha(x,y)$ is sampled at exactly the same location (x,y) but is weighted differently at each spatial frequency (υ,ω). The different spatial-frequency responses for obtaining each of the $\mathcal{A}$ images is obtained by changing the size of an adjustable, varying optical aperture 10 of a single image gathering device 12 for each acquired image. The scene and the imager must be stationary with respect to one another.

The image-gathering process transforms the continuous radiance field $L(x,y)$ reflected or emitted by the target into $\mathcal{A}$ discrete sample signals, each acquired by a different optical response $\tau_\alpha(x,y)$ on the same sampling lattice $\underline{|||}$. The optical response $\tau_\alpha(x,y)$ is the convolution of the objective lens point spread function and the photosensor point spread function for the α'th optical aperture opening.

Each acquired signal $s_\alpha(x,y)$, $\alpha = 1, 2..., \mathcal{A}$ is given by

$$s_\alpha(x,y) = [K_\alpha L(x,y) * \tau_\alpha(x,y)]\underline{|||} + n_\alpha(x,y), \tag{1a}$$

where each successive signal $s_\alpha(x,y), \alpha = 1, 2, ..., \mathcal{A}$, is acquired with a different optical response $\tau_\alpha(x,y)$, K_α is the steady-state gain of the linear radiance-to-signal conversion, $n_\alpha(x,y)$ is the additive discrete photodetector noise, and $\underline{|||} \equiv \underline{|||}(x,y)$ is the uniform rectangular sampling lattice with a unit sampling interval in each dimension. Thus, each signal $s_\alpha(x,y)$ is sampled at exactly the same location (x,y) but is weighted differently at each spatial frequency (υ,ω). As stated above

this process can be implemented by widening the objective lens aperture (i.e., increasing its diffraction limit) for each successive image. The Fourier transform of this process is

$$\hat{s}_\alpha(\upsilon,\omega) = \left[K_\alpha\, \widehat{L}(\upsilon,\omega)\hat{\tau}_\alpha(\upsilon,\omega)\right] * \underline{\underline{\hat{|||}}} + \hat{n}_\alpha(\upsilon,\omega) \tag{1b}$$

or, more explicitly,

$$\begin{bmatrix} \hat{s}_1(\upsilon,w) \\ \hat{s}_2(\upsilon,\omega) \\ \vdots \\ \hat{s}_\alpha(\upsilon,\omega) \\ \vdots \\ \hat{s}_{\mathcal{A}}(\upsilon,\omega) \end{bmatrix} = \begin{bmatrix} \cdots & K_1\hat{\tau}_1(\upsilon,\omega) & K_1\hat{\tau}_1(\upsilon+1,\omega) & K_1\hat{\tau}_1(\upsilon,\omega+1) & \cdots \\ \cdots & K_2\hat{\tau}_2(\upsilon,\omega) & K_2\hat{\tau}_2(\upsilon+1,\omega) & K_2\tau_2(\upsilon,\omega+1) & \cdots \\ & & \vdots & & \\ \cdots & K_\alpha\hat{\tau}_\alpha(\upsilon,\omega) & K_\alpha\hat{\tau}_\alpha(\upsilon+1,\omega) & \cdots & \\ & & \vdots & & \\ \cdots & K_{\mathcal{A}}\hat{\tau}_{\mathcal{A}}(\upsilon,\omega) & K_{\mathcal{A}}\hat{\tau}_{\mathcal{A}}(\upsilon+1,\omega) & K_{\mathcal{A}}\hat{\tau}_{\mathcal{A}}(\upsilon,\omega+1) & \cdots \end{bmatrix} \begin{bmatrix} \vdots \\ \hat{L}(\upsilon,\omega-1) \\ \hat{L}(\upsilon-1,\omega) \\ \hat{L}(\upsilon,\omega) \\ \hat{L}(\upsilon+1,\omega) \\ \hat{L}(\upsilon,\omega+1) \\ \vdots \end{bmatrix} + \begin{bmatrix} \hat{n}_1(\upsilon,\omega) \\ \hat{n}_2(\upsilon,\omega) \\ \vdots \\ \hat{n}_\alpha(\upsilon,\omega) \\ \vdots \\ \hat{n}_{\mathcal{A}}(\upsilon,\omega) \end{bmatrix}, \tag{1c}$$

where $\mathcal{A}$ equals the number of sidebands that the process restores. The associated restoration passband for $|\widehat{B}_s| = 1$ increases to

$$\widehat{B}_{\mathcal{A}} = \left\{(\upsilon,\omega); |\upsilon| \le \frac{\sqrt{\mathcal{A}}}{2}, |\omega| \le \frac{\sqrt{\mathcal{A}}}{2}\right\} \tag{1d}$$

with area $|\widehat{B}_{\mathcal{A}}| = \mathcal{A}|\widehat{B}_s| = \mathcal{A}$.

FIGS. 4(a), 4(b) and 4(c) depict typical spatial-frequency responses $\hat{\tau}_\alpha(\upsilon,\omega)$ relative to sampling passband $\widehat{\mathcal{B}}_s$ in one dimension for convenience, wherein $\mathcal{A}$ is respectively equal to 1, 4 and 9.

The image-restoration process restores a continuous image from the $\mathcal{A}$ discrete signals $s_\alpha(x,y)$. The Fourier transform of the image is given by the expression

$$\widehat{R}_{\mathcal{A}}(\upsilon,\omega) = \sum_{\alpha=1}^{\mathcal{A}} K_\alpha^{-1}\widehat{\Psi}_\alpha(\upsilon,\omega)\ \hat{s}_\alpha(\upsilon,\omega). \tag{2}$$

The Wiener-matrix filter $\widehat{\Psi}_\alpha(\upsilon,\omega)$ which minimizes the mean square difference between $L(x,y)$ and $R_{\mathcal{A}}(x,y)$ is

$$\widehat{\Psi}_\alpha(\upsilon,\omega) = \sum_{\beta=1}^{\mathcal{A}} \widehat{\Phi}_L(\upsilon,\omega)\, \hat{\tau}^*_\beta(\upsilon,\omega) \left[\widehat{T}^{-1}(\upsilon,\omega)\right]_{\beta\alpha}, \tag{3}$$

where

$$\left[\widehat{T}(\upsilon,\omega)\right]_{\alpha\beta} = \left[\widehat{\Phi}_L(\upsilon,\omega)\, \hat{\tau}_\alpha(\upsilon,\omega)\, \hat{\tau}^*_\beta(\upsilon,\omega)\right] * \underline{\hat{|||}} + \widehat{\Phi}_{N_\alpha}(\upsilon,\omega)\, \delta(\alpha,\beta).$$

For white noise with variance $\sigma^2_{N_\alpha}$

$$\left[\widehat{T}(\upsilon,\omega)\right]_{\alpha\beta} = \left[\widehat{\Phi}'_L(\upsilon,\omega)\, \hat{\tau}_\alpha(\upsilon,\omega)\, \hat{\tau}^*_\beta(\upsilon,\omega)\right] * \underline{\hat{|||}} + (K_\alpha\sigma_L/\sigma_{N_\alpha})^{-2}\, \delta(\alpha,\beta).$$

Dropping for convenience the spatial-frequency dependence (υ,ω), the matrix $[\widehat{T}(\upsilon,\omega)]$ is given more explicitly by

$$\left[\widehat{T}\right] = \begin{bmatrix} \left(\widehat{\Phi}'_L \hat{\tau}_1 \hat{\tau}^*_1\right) * \underline{\hat{|||}} + (K_1\sigma_L/\sigma_{N_1})^{-2} & \cdots\cdots & \left(\widehat{\Phi}'_L \hat{\tau}_1 \hat{\tau}^*_{\mathcal{A}}\right) * \underline{\hat{|||}} \\ \left(\widehat{\Phi}'_L \hat{\tau}_2 \hat{\tau}^*_1\right) * \underline{\hat{|||}} & \cdots\cdots & \left(\widehat{\Phi}'_L \hat{\tau}_2 \hat{\tau}^*_{\mathcal{A}}\right) * \underline{\hat{|||}} \\ \cdots\cdots & \left(\widehat{\Phi}'_L \hat{\tau}_\alpha \hat{\tau}^*_\alpha\right) * \underline{\hat{|||}} + (K_\alpha\sigma_L/\sigma_{N_\alpha})^{-2} & \cdots\cdots \\ \left(\widehat{\Phi}_L \hat{\tau}_{\mathcal{A}} \hat{\tau}^*_1\right) * \underline{\hat{|||}} & \cdots\cdots & \left(\widehat{\Phi}'_L \hat{\tau}_{\mathcal{A}} \hat{\tau}^*_{\mathcal{A}}\right) * \underline{\hat{|||}} + (K_{\mathcal{A}}\sigma_L/\sigma_{N_{\mathcal{A}}})^{-2} \end{bmatrix}.$$

The corresponding minimum mean square restoration error power spectral density is

$$\widehat{\epsilon}^2_{LR\mathcal{A}}(\upsilon,\omega) = \widehat{\Phi}_L(\upsilon,\omega)\left[1 - \widehat{\Gamma}_{\mathcal{A}}(\upsilon,\omega)\right], \tag{4}$$

where

$$\widehat{\Gamma}_{\mathcal{A}}(\upsilon,\omega) = \sum_{\alpha=1}^{\mathcal{A}} \hat{\tau}_\alpha(\upsilon,\omega)\widehat{\Psi}_\alpha(\upsilon,\omega) \tag{5}$$

is the throughput response for multiresponse imaging.

FIGS. 5(a), 5(b) and 5(c) depict typical throughput responses $\widehat{\Gamma}(\upsilon,\omega)$ where $\mathcal{A} = 1$, 4 and 9, respectively, with SNR = 256. As shown, the throughput responses improve relative to the sampling passband as $\mathcal{A}$ increases.

FIGS. 6(a) and 7(a) illustrate two targets – a random multiple polygon target and a resolution wedge target. The mean distance μ between the edges of the polygons is equal to 0.75 relative to the unit sampling interval of the imager.

FIGS. 6(b) and 7(b) illustrate images restored for a single (conventional) image-gathering event; FIGS. 6(c) and 7(c) illustrate images restored for $\mathcal{A} = 4$ image-gathering events; and FIGS. 6(d) and 7(d) illustrate images stored for $\mathcal{A} = 9$ image-gathering processes. The improvement in resolution shown in FIGS. 6(c), 7(c), 6(d) and 7(d) over that shown in FIGS. 6(b) and 7(b) is a direct consequence of this invention.

Many improvements, modifications and substitutions will be apparent to the skilled artisan without departing from the spirit and scope of the present invention as described herein and defined in the following claims.

MULTIRESPONSE IMAGE GATHERING AND PROCESSING FOR IMPROVED RESOLUTION

Abstract of the Disclosure

The implementation of this invention consists of two elements, the image-gathering device and an image-restoration filter algorithm. The image- gathering device is implemented with an optical aperture control that allows one to change the spatial-frequency response of the image-gathering device for each one of the successive image acquisitions, and the image-restoration algorithm unscrambles the within-passband and aliased signal components in the presence of photosensor noise to produce an image with an increased resolution. The upper limit of the increase in resolution is $1/\sqrt{\mathcal{A}}$ times the sampling interval of the image-gathering device for $\mathcal{A}$ image-gathering events. The image-gathering device and the target must be stationary with respect to each other during the image-gathering process.

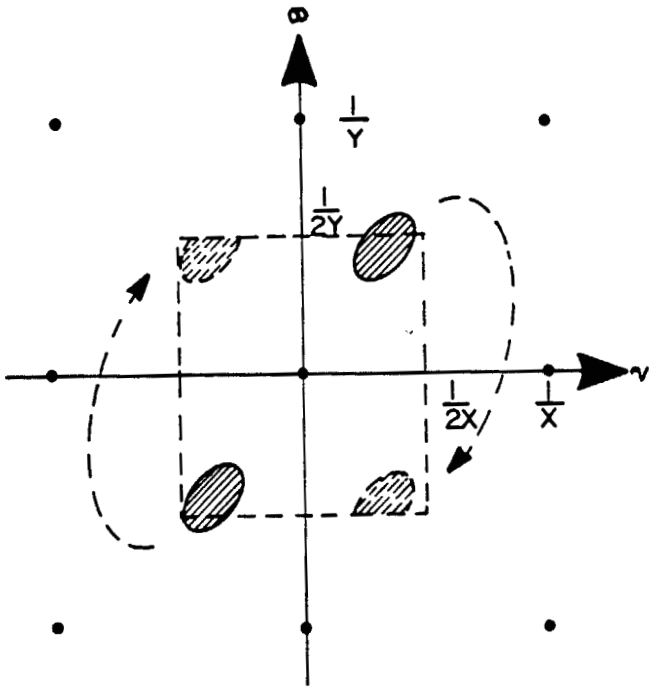

FIG. 1(a)

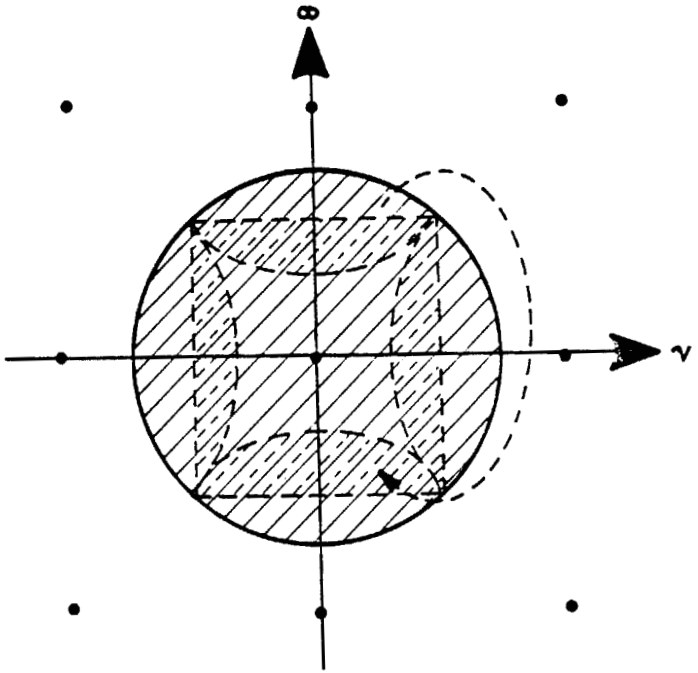

FIG. 1(b)

0218551 714
05/14/92

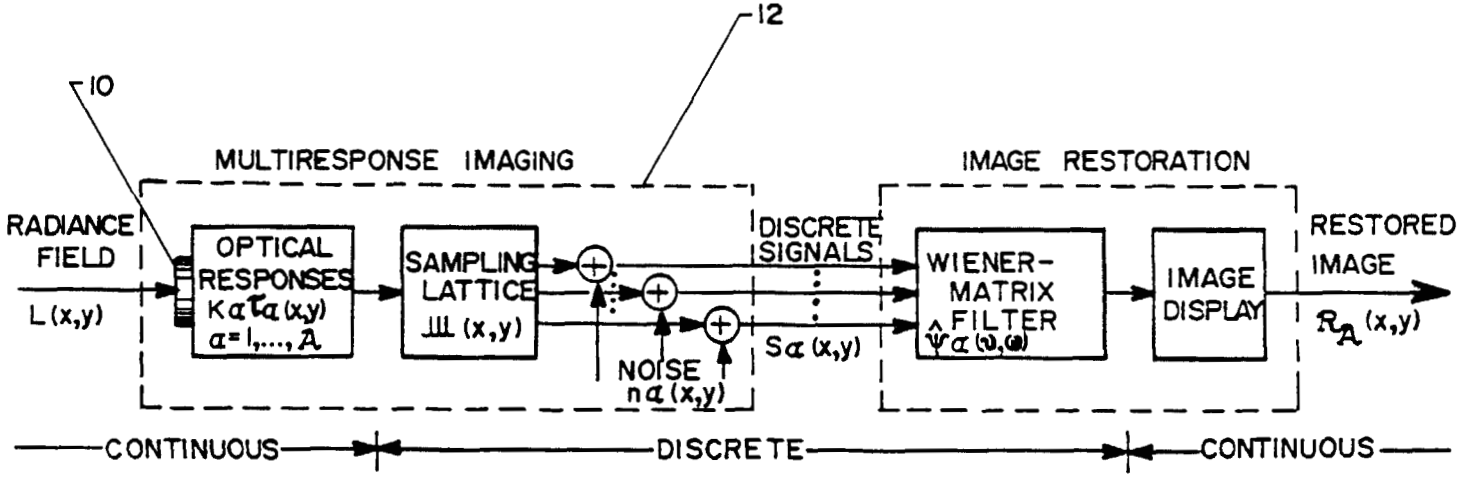
12
10
MULTIRESPONSE IMAGING
IMAGE RESTORATION
RADIANCE FIELD
L(x,y)
OPTICAL RESPONSES
Kα τα(x,y)
α=1,...,A
SAMPLING LATTICE
(x,y)
NOISE
nα(x,y)
DISCRETE SIGNALS
Sα(x,y)
WIENER-MATRIX FILTER
ψ̂α(ω,ω)
IMAGE DISPLAY
RESTORED IMAGE
RA(x,y)
CONTINUOUS
DISCRETE
CONTINUOUS

FIG. 2

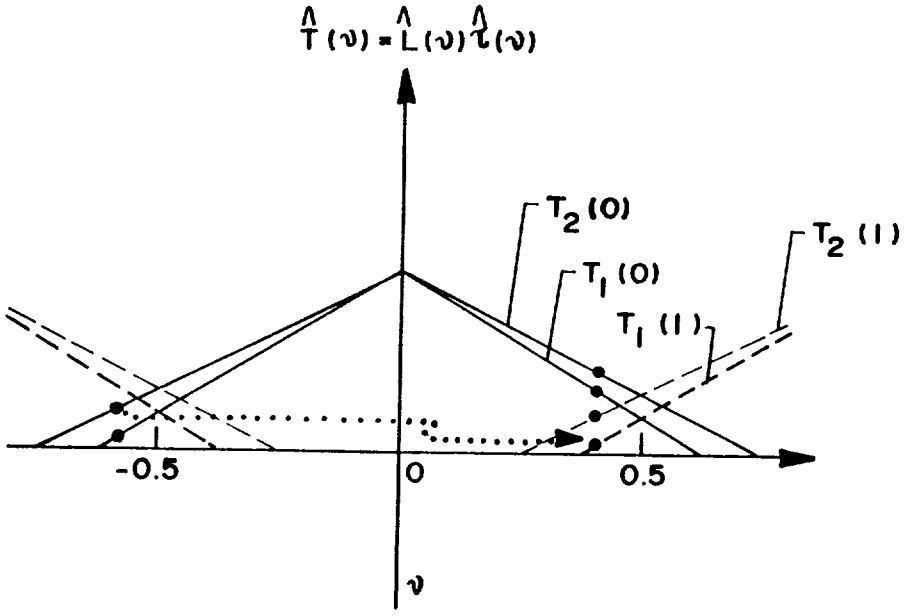

FIG. 3

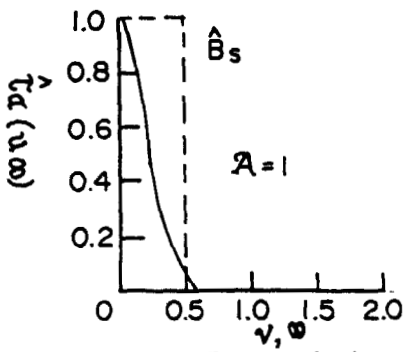

FIG. 4(a)

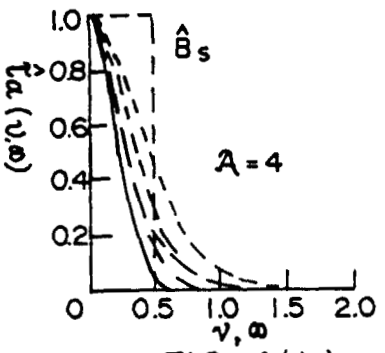

FIG. 4(b)

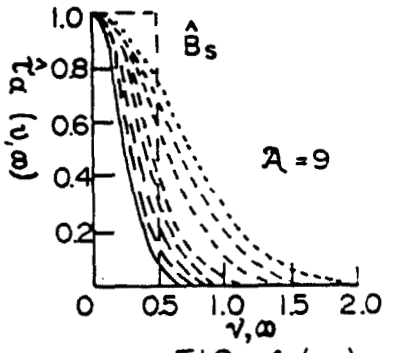

FIG. 4(c)

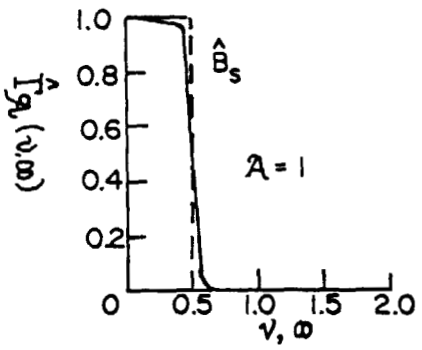

FIG. 5(a)

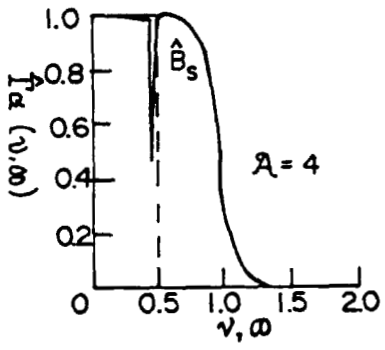

FIG. 5(b)

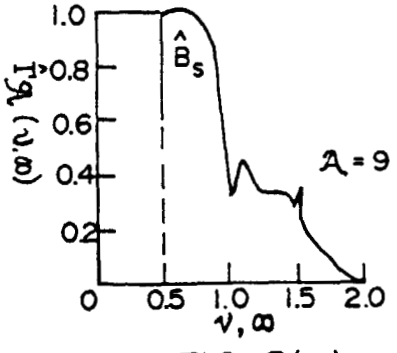

FIG. 5(c)

FIG. 6(a)

FIG. 6(b)

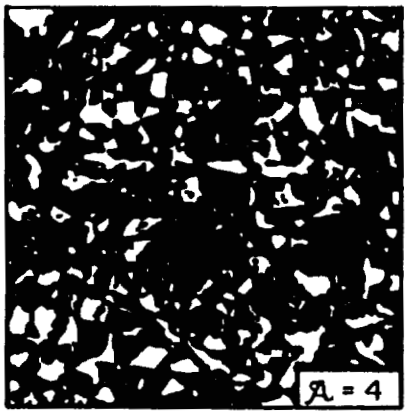

FIG. 6(c)

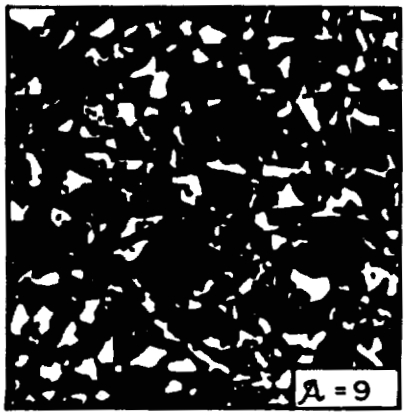

FIG. 6(d)

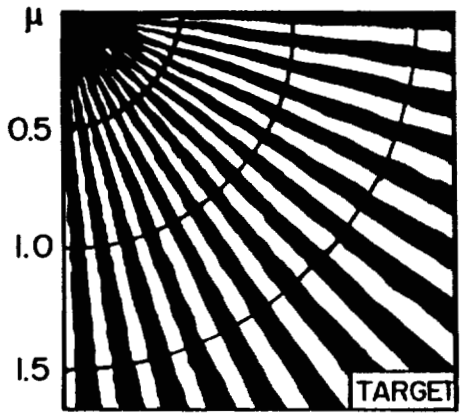

FIG. 7(a)

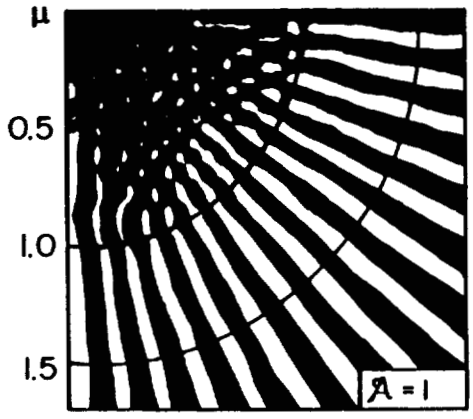

FIG. 7(b)

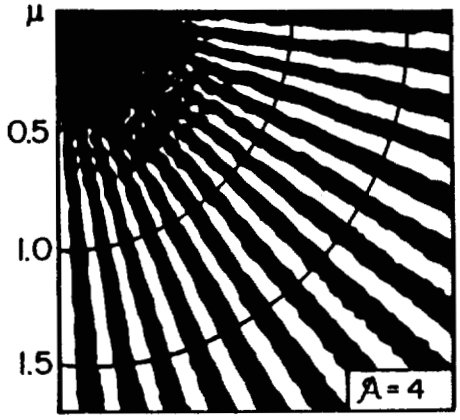

FIG. 7(c)

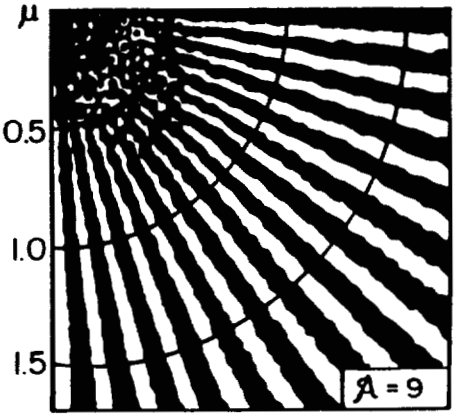

FIG. 7(d)